Catalysis Communications 11 (2010) 391–395

Contents lists available at ScienceDirect

Catalysis Communications

journal homepage: www.elsevier.com/locate/catcom

# Increased surface area of unsupported $Mo_2C$ catalyst by alkali-treatment

Liang Zhao [a,b], Farnaz Sotoodeh [b], Kevin J. Smith [b,*]

[a] State Key Laboratory of Heavy Oil Processing, China University of Petroleum, Beijing, Changping 102249, China
[b] Department of Chemical and Biological Engineering, University of British Columbia, 2360 East Mall, Vancouver, BC, Canada V6T 1Z3

ARTICLE INFO

*Article history:*
Received 3 September 2009
Received in revised form 4 November 2009
Accepted 10 November 2009
Available online 13 November 2009

*Keywords:*
Catalyst
Catalyst preparation
Alkali-treatment
$Mo_2C$
Tetrahydrocarbazole dehydrogenation
Synthesis gas

ABSTRACT

A 50% increase in the surface area of an unsupported $Mo_2C$ catalyst, prepared by temperature-programmed reduction of a $MoO_3$ precursor using $CH_4/H_2$, is reported following treatment in 5 M NaOH at 363 K for 2–12 h. The treated catalyst showed an increase in pores of size <3 nm and an increase in activity for the dehydrogenation of 1,2,3,4-tetrahydrocarbazole and the hydrogenation of CO, compared to the un-treated $Mo_2C$.



## 1. Introduction

Molybdenum carbide is known to have catalytic properties similar to those of noble metals. Consequently, there is a significant interest in $Mo_2C$ as a catalyst for a wide range of reactions, including hydrogenation [1,2], dehydrogenation [3–6], synthesis gas conversion [7,8], hydrocarbon isomerization [9], water–gas-shift [10] and hydrogen production from methanol and ethanol [11]. Several methods have been developed for the synthesis of $Mo_2C$, including the most often used temperature-programmed reduction (TPR) of oxide precursors using $CH_4$ or $CH_4/H_2$ mixtures [12]. Other approaches have also been reported such as TPR using butane [13], carbothermal hydrogen reduction [14], the pyrolysis of metal precursors [15], solution reactions [16], and photochemically promoted formation of carbide from metallic molybdenum and graphite [17].

The goal of almost all these synthesis methods is to enhance the catalyst surface area and hence increase the activity of $Mo_2C$ catalysts. However, some of the known preparation methods are subject to limitations associated with cost and convenience. Furthermore, the surface area of the $Mo_2C$ produced by temperature-programmed reduction of oxide precursors is greatly influenced by preparation conditions. The temperature ramp rate, the flow rate and composition of the reducing gas ($CH_4$, $C_2H_6$, $H_2$), and the precursor, all impact the product surface area and consequently, reported surface areas of unsupported $Mo_2C$ vary widely [1–14,18–20]. An alternative, simple method of producing high surface area $Mo_2C$ would be of significant benefit.

Alkali-treatment is a well known post-treatment technique used in zeolite synthesis, which introduces mesopore and macropore structure to the zeolite pore system [21–25]. The alkali-treated zeolites show higher catalytic activity and increased surface area compared to un-treated zeolites. Although this technique has been used to prepare high surface area zeolites [21–25] it has not been applied to $Mo_2C$ catalysts.

In the present study, we report a simple post-treatment of $Mo_2C$ using a hot alkali solution that enhances the $Mo_2C$ surface area while retaining the structural integrity of the $Mo_2C$. The obtained high surface area $Mo_2C$ has been used as a catalyst for the dehydrogenation of 1,2,3,4-tetrahydrocarbazole (THCZ) and the hydrogenation of CO. THCZ is a candidate heteroaromatic compound for hydrogen storage. Hydrogen is released through catalytic dehydrogenation at low temperature ($\leqslant$423 K), using platinum group metal catalysts (Pd, Pt, Rh and Ru) [26–28]. Because of the cost of the platinum group metals, metal carbides are possible alternatives for this reaction. Metal carbides have also been shown to be active in several CO hydrogenation reactions aimed at producing higher hydrocarbons [18] and alcohols [29–31] and consequently we have tested the prepared $Mo_2C$ for syngas conversion as well.

## 2. Experimental

### 2.1. Catalyst preparation

Unsupported $Mo_2C$ was synthesized by temperature-programmed reduction of an oxide precursor. Approximately 3 g of $MoO_3$ ($MoO_3$, +99.5%, Sigma–Aldrich) was placed in a quartz

* Corresponding author. Tel.: +1 604 822 3601; fax: +1 604 822 6003.
*E-mail address:* kjs@interchange.ubc.ca (K.J. Smith).

1566-7367/$ - see front matter © 2009 Elsevier B.V. All rights reserved.
doi:10.1016/j.catcom.2009.11.008

tubular reactor and heated at a rate of 5 K/min from room temperature to 573 K, followed by heating at a rate of 1 K/min from 573 K to 948 K in 100 ml(STP)/min of $CH_4/H_2$ (1:4 vol). The final temperature was held for 2 h in the same $CH_4/H_2$ flow. The sample was then rapidly cooled to room temperature in a 80 ml(STP)/min flow of $H_2$. The sample was passivated by exposure to a mixture of 1% $O_2$ in He at a flow rate of 133 ml(STP)/min for 4 h before being removed from the reactor.

Approximately 3 g of the passivated $Mo_2C$ was placed in 90 ml of a 5 M NaOH solution and stirred for 2, 6 and 12 h at 363 K. The mixture was subsequently cooled in an ice bath. The liquid and solid were separated by centrifuging at 12,000 rpm for 20 min at 288 K. The solid was washed with de-ionized water until the washings showed a neutral pH. The catalyst was then dried at room temperature and activated in $H_2$ (5–10 ml(STP)/min) at 573 K for 2 h before being used for reaction. The catalysts are designated AT-2, AT-6 and AT-12 to identify the duration of the alkali-treatment in each case.

### 2.2. Characterization

The passivated catalysts were characterized by powder X-ray diffraction (XRD), scanning electron microscopy (SEM), energy dispersive X-ray analysis (EDX), $N_2$-adsorption/desorption at 77 K and thermogravimetric analysis. Prior to $N_2$ adsorption, the samples were degassed at 423 K in 30 mol% $N_2$/He (15 ml(STP)/min) for 2 h to remove moisture. All other analyses were carried out on the passivated samples without further treatment. The XRD analysis was performed using a Siemens D500 Cu Kα X-ray source of wavelength ($\lambda$) 1.54 Å. The scan rate was 2° per min for a range of 5–80° to confirm the structure of $Mo_2C$, and 0.5° per min for the range of 32–42° to estimate the crystallite size ($d_c$) of the $Mo_2C$ using the Scherrer equation, $d_c = K\lambda/\beta\cos\theta$, where the constant $K$ was taken to be 0.9, $\lambda$ is the wavelength of radiation, $\beta$ is the peak width in radians and $\theta$ is the angle of diffraction. $N_2$-adsorption/desorption isotherms were recorded at 77 K using a Micromeritics ASAP 2020 analyzer. The total surface area was calculated according to the BET isotherm, and the micropore volume, the mesopore volume, and external surface area were evaluated by the *t*-plot method. The pore size was reported as the average pore diameter. SEM/EDX analysis was performed using a Hitachi S-3000 N electron microscope operated with a 150 kV electron beam acceleration voltage. Thermogravimetric analysis of the catalysts was done using a TGA-50 thermogravimetric analyzer (Shimadzu, Japan). About 5–10 mg of the catalyst was loaded into an alumina crucible and heated to 1000 K at a rate of 5 K/min in an air atmosphere (flow rate = 15 ml(STP)/min). The weight gain and loss were quantified and differential TGA (DTG) was accomplished using standard TGA software.

### 2.3. Catalyst activity

Dehydrogenation of 1,2,3,4-tetrahydrocarbazole (THCZ) was performed at 423 K using a solution of 2.0 g THCZ dissolved in 30 ml mesitylene. The solution was loaded into a 50 ml glass flask reactor. The 1.0 g alkali-treated $Mo_2C$ was added to the solution after activation in hydrogen. The reactor was sealed, stirred, purged in a flow of He (100 ml(STP)/min) and heated to 423 K. The He was used as a carrier gas for continuous removal of the produced hydrogen and the exit gas composition was continuously monitored using a quadrupole mass spectrometer. Catalyst activity was determined by the production of $H_2$ and confirmed by periodic liquid analysis using a gas chromatograph (Shimadzu GC14A) with a flame ionization detector and an ATTM-5 25 M × 0.53 mm capillary column. Product identities were also confirmed by a Shimadzu QP-2010S GC/MS using a Restek RTX5 30 M × 0.25 mm capillary column. The absence of internal and external mass transfer effects on the reaction was confirmed experimentally and by theoretical analysis [32].

The activity of the $Mo_2C$ catalysts for synthesis gas conversion was also measured using a laboratory fixed-bed micro reactor (o.d. = 9.53 mm and i.d. = 6.35 mm, copper lined stainless steel tube). The catalyst particles were placed on a packed bed of quartz wool inside the reactor and held in place by a bed of quartz beads. The catalyst bed depth was 5–7 cm and calculation showed that this configuration ensured plug-flow through the reactor. Synthesis gas ($H_2$:CO = 1) was reacted at 573 K, a pressure of 8.3 MPa and a GHSV = 3960 $h^{-1}$. A high temperature back pressure regulator was used to control the reactor pressure. The reaction products were analyzed using an in-line gas chromatograph (GC). Light gases (CO, $CO_2$ and $C_1$–$C_4$ hydrocarbons) were separated using a 5 m temperature-programmed Porapak Q 80/100 packed column and quantified with a thermal conductivity detector. The alcohols, aldehydes, ketones, carboxylic acids and $C_5$ + hydrocarbons were separated using a 30 m temperature-programmed EC™-wax capillary column (i.d. = 0.53 mm and film thickness 1.20 μm) and quantified using a flame ionization detector. GC/MS analysis was also completed periodically to confirm the identity of the reactor products. Analysis of several repeat experiments showed the conversion and selectivity data to be within ±10% of the reported values. Calculation of the internal and external heat and mass transfer rates, and application of the Mears and Weisz–Prater criteria, confirmed that at the conditions of the experiments, the reactor operated free of significant heat and mass transfer resistances.

## 3. Results and discussion

### 3.1. $Mo_2C$ properties

The properties of the $Mo_2C$ and the alkali-treated $Mo_2C$, reported in Table 1, show that several changes occurred to the $Mo_2C$ after alkali-treatment. Compared to the un-treated $Mo_2C$, the alkali-treated $Mo_2C$ showed a significant increase in surface area, an increase in the micropore area and a decrease in the average pore size of the $Mo_2C$. The BET surface area of the alkali-treated $Mo_2C$ increased from 29 $m^2/g$ to 40–47 $m^2/g$, an increase of about 50%. The $N_2$ adsorption and desorption isotherms of the $Mo_2C$ and the alkali-treated $Mo_2C$ (Fig. 1) showed increased hysteresis effects with increased time of the alkali-treatment. Fig. 2 presents the pore size distribution of the $Mo_2C$ and the alkali-treated $Mo_2C$. Clearly, the alkali-treatment increased the fraction of pores <3 nm in size and decreased the average pore size ($d_p$) of the $Mo_2C$ treated with NaOH for 2 and 6 h. After 12 h, Fig. 2 shows that

**Table 1**
Properties of the unsupported $Mo_2C$ catalysts.

| Property | $Mo_2C$ | Alkali-treated $Mo_2C$[a] | | |
|---|---|---|---|---|
| | | 2 h AT-2 | 6 h AT-6 | 12 h AT-12 |
| *$N_2$ adsorption–desorption* | | | | |
| $S_{BET}$ ($m^2/g$) | 29.4 ± 1.1[b] | 44.5 | 47.3 ± 3.1[b] | 40.0 |
| $S_{t\text{-micro}}$ ($m^2/g$) | 0.06 ± 0.05 | 0.05 | 4.8 ± 2.5 | 10.4 |
| $S_{t\text{-ext}}$ ($m^2/g$) | 29.9 ± 1.9 | 44.4 | 42.5 ± 0.6 | 29.6 |
| $V_p$ ($cm^3/g$) | 0.031 ± 0.005 | 0.043 | 0.036 ± 0.001 | 0.030 |
| $d_p$ (nm) | 4.19 ± 0.5 | 3.82 | 3.01 ± 0.12 | 2.98 |
| *XRD analysis* | | | | |
| $d_c$ (1 0 1) (nm) | 13.6 | 13.0 | 13.1 | 13.9 |
| $d_c$ (1 0 0) (nm) | 15.2 | 14.5 | 15.2 | 14.6 |
| *a* (Å) | 3.005 | 3.005 | 3.009 | 3.012 |
| *c* (Å) | 4.742 | 4.782 | 4.764 | 4.746 |

[a] $Mo_2C$ treated in 5 M NaOH for the time period shown.
[b] Standard deviation from three repeat measurements.

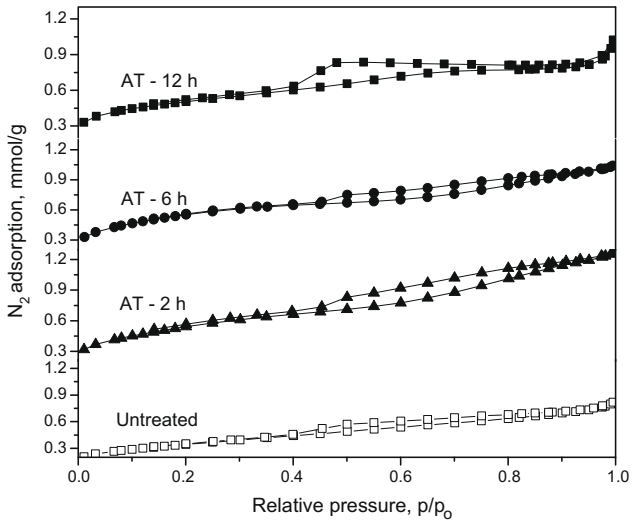


**Fig. 1.** $N_2$ adsorption–desorption isotherms measured at 77 K for $Mo_2C$ and alkali-treated $Mo_2C$ catalysts.

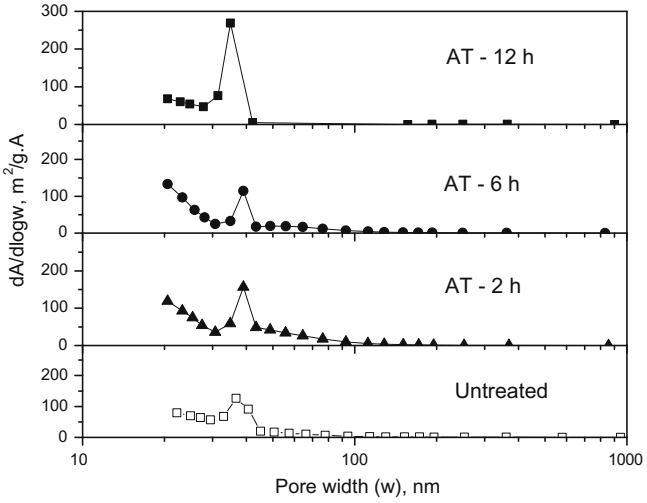


**Fig. 2.** Pore size distribution of $Mo_2C$ and alkali-treated $Mo_2C$ catalysts.

a significant increase in pores of size 20–30 nm had also occurred. The data of Table 1 shows that as the alkali-treatment time increased, the micropore area also increased. These results suggest that the alkali-treatment initially removed material from the $Mo_2C$ to generate new pores of <3 nm in diameter, resulting in a decrease in the average pore size. With increased treatment time (12 h) the removal of material from larger pores also occurred. These observations are quite different to changes observed in zeolites treated with alkali. Typically with zeolites, the microporosity decreases and the meso- and macroporosity increases, leading to an increase in the average pore size of the alkali-treated zeolite compared to the un-treated zeolite [21–25].

Fig. 3 shows the XRD patterns of the $Mo_2C$ and the alkali-treated $Mo_2C$. The eight peaks at $2\theta$ equal to 34.48, 37.96, 39.52, 52.28, 61.76, 69.56, 74.80, and 75.72 can be indexed to hexagonal $Mo_2C$(1 0 0), (0 0 2), (1 0 1), (1 0 2), (1 1 0), (1 0 3), (1 1 2), and (2 0 1). There were no differences between the peaks before and after alkali-treatment, indicating that the crystal structure of the $Mo_2C$ was not changed by the alkali-treatment. The $Mo_2C$ crystallite size was calculated from the Scherrer equation and the results, summarized in Table 1, suggest that no significant change in crys-

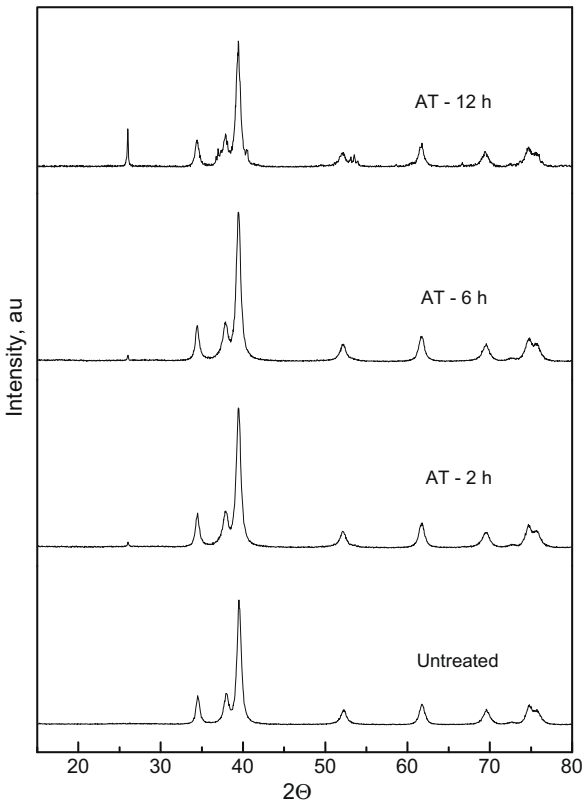


**Fig. 3.** X-ray diffractograms of $Mo_2C$ and alkali-treated $Mo_2C$ catalysts.

tallite size occurred after alkali-treatment of the $Mo_2C$ either. The lattice parameters of the catalysts were also calculated using the Bragg equation and the results are listed in Table 1. According to the JCPDS card No. 11-0680, the lattice parameters of $Mo_2C$ are $a$ = 3.006 Å and $c$ = 4.733 Å and the results obtained in the present work (Table 1) are in good agreement with these values. Hence we conclude that the crystal structure of the $Mo_2C$ was not affected by alkali-treatment. Also, the SEM micrographs of Fig. 4 show that the $Mo_2C$ and the alkali-treated $Mo_2C$ had very similar macro-morphology. The materials consisted of platelet-like grains, <5 μm in size, and the alkali-treatment had no discernable effect on this $Mo_2C$ morphology.

Fig. 5 shows the differential TGA curves of the $Mo_2C$ and the 2 h alkali-treated $Mo_2C$. Both samples had very similar characteristics, with two main peaks generated as the $Mo_2C$ was oxidized to $MoO_2$ and then $MoO_3$. The total weight gain in both cases was 95% of the expected gain for pure $Mo_2C$ conversion to $MoO_3$, confirming that the bulk of the material was phase pure $Mo_2C$. These results indicate that the new pores of <3 nm diameter generated by alkali-treatment were a consequence of $Mo_2C$ dissolution, rather than simply due to the selective removal of excess carbon or other impurity from the pores of the catalyst.

### 3.2. THCZ dehydrogenation

Since THCZ is a solid powder at ambient conditions with high boiling point (598 K) and melting point (391 K), the dehydrogenation reaction was carried out in the liquid phase by dissolving the THCZ in mesitylene. Over supported Pd catalysts, the reaction was zero-order in substrate (THCZ) concentration, and the catalysts showed 100% selectivity to the desired carbazole product. However, it was shown from experiment that product inhibition slowed the rate of reaction and 81% conversion was obtained after about

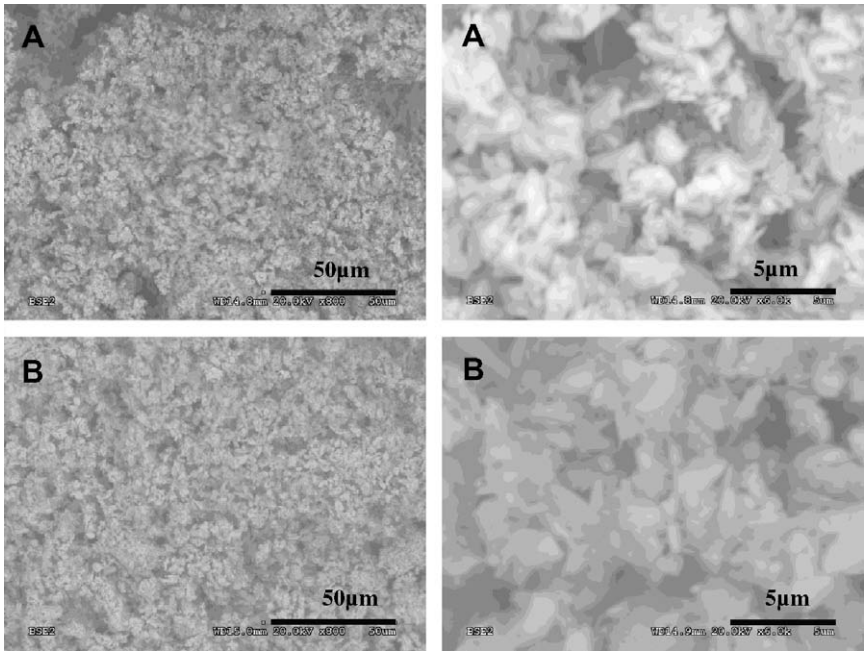


**Fig. 4.** SEM micrographs of (A) $Mo_2C$ and (B) 2 h alkali-treated $Mo_2C$.

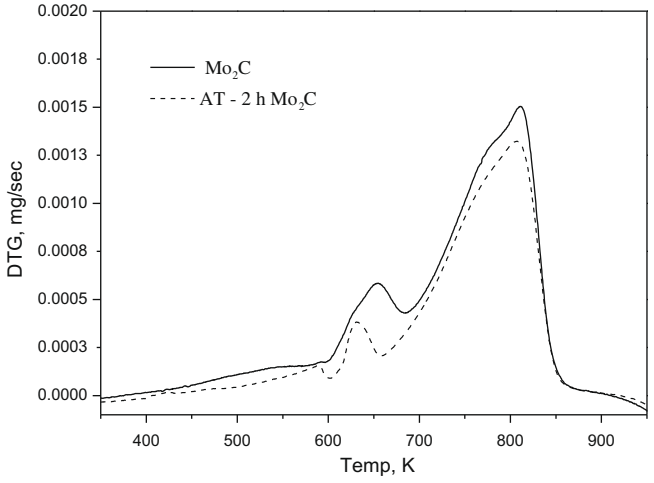


**Fig. 5.** Temperature-programmed oxidation of $Mo_2C$ and 2 h alkali-treated $Mo_2C$ catalysts.

27 h at 101 kPa and 413 K. The initial rate of THCZ dehydrogenation at these conditions was 10 mM $g_{cat}^{-1}$ $min^{-1}$ [26,27].

The dehydrogenation activity of $Mo_2C$ and the 2 h alkali-treated $Mo_2C$ was determined at 423 K. The data for the two catalysts presented in Table 2, show an initial THCZ dehydrogenation rate of 0.014 and 0.048 mM $g_{cat}^{-1}$ $min^{-1}$, respectively. The alkali-treated $Mo_2C$ had about 3×'s the initial activity of the un-treated $Mo_2C$ for THCZ conversion. The $H_2$ produced in the first 30 min of reaction was similarly higher on the alkali-treated catalyst. The activity (on a mass basis) of both $Mo_2C$ catalysts was approximately two orders of magnitude lower than that reported for supported Pd catalysts used for the dehydrogenation reaction.

**Table 2**
THCZ dehydrogenation activity measured in a batch reactor at 101 kPa and 423 K over unsupported $Mo_2C$ catalysts.

| Catalyst | Reaction temperature (K) | Initial rate (mM $g_{cat}^{-1}$ $min^{-1}$)[a] | $H_2$ produced/$g_{cat}$ (mmol/$g_{cat}$)[a] |
|---|---|---|---|
| $Mo_2C$ | 423 | 0.014 | 0.056 |
| AT-2 $Mo_2C$ | 423 | 0.048 | 0.184 |

[a] After 30 min reaction.

### 3.3. CO hydrogenation reaction

Several Mo compounds have also been investigated for synthesis gas conversion. $MoS_2$, $Mo_2O_3$ and $Mo_2C$ show high selectivity towards liquid oxygenates, especially ethanol, when doped with alkali earth metals. In addition, the $Mo_2C$ has high $CO_2$ yield rather than water, a consequence of high water–gas-shift activity [10]. For example, the rate of CO consumption over $Mo_2C$ with low surface area (approximately 5 $m^2/g$) at 573 K and 8.0 MPa with a $H_2$:CO ratio 1:1, was approximately 0.4 mmol $gcat^{-1}$ $min^{-1}$ based on a reported CO conversion of 58% at a GHSV of 2000 $h^{-1}$ [29]. In the present work, $Mo_2C$ and the 2 h alkali-treated $Mo_2C$ were tested for synthesis gas conversion at 573 K and 8.0 MPa with a $H_2$:CO ratio 1:1 and a GHSV of 3960 $h^{-1}$. The initial catalyst activities (after a 2 h stabilization period) are reported in Table 3. The data show that alkali-treated $Mo_2C$ increased the CO consumption rate by about 10% compared to the un-treated $Mo_2C$. The data show higher CO consumption rates than that reported by Xiang et al. [29–31] on both the $Mo_2C$ and the alkali-treated $Mo_2C$. High $CH_4$ and $CO_2$ selectivities were also obtained on the two catalysts of the present study. Typically, $Mo_2C$ catalysts are promoted with

**Table 3**
Syngas conversion on $Mo_2C$ and alkali-treated $Mo_2C$. Reaction conditions: pressure = 8.2 MPa, temperature = 573 K, CO:$H_2$ = 1 and GHSV = 3960 $h^{-1}$.

| Catalyst | Initial CO consumption rate (mmol $g_{cat}^{-1}$ $min^{-1}$)[a] | Initial product selectivity[a] | | |
|---|---|---|---|---|
| | | $CO_2$ | $CH_4$ | $C_2$ + alcohols and HC's |
| | | C atom% | | |
| $Mo_2C$ | 2.06 | 48.6 | 26.0 | 25.4 |
| AT-2 $Mo_2C$ | 2.24 | 51.7 | 20.9 | 27.5 |

[a] Measured 2 h after the start of the experiment.

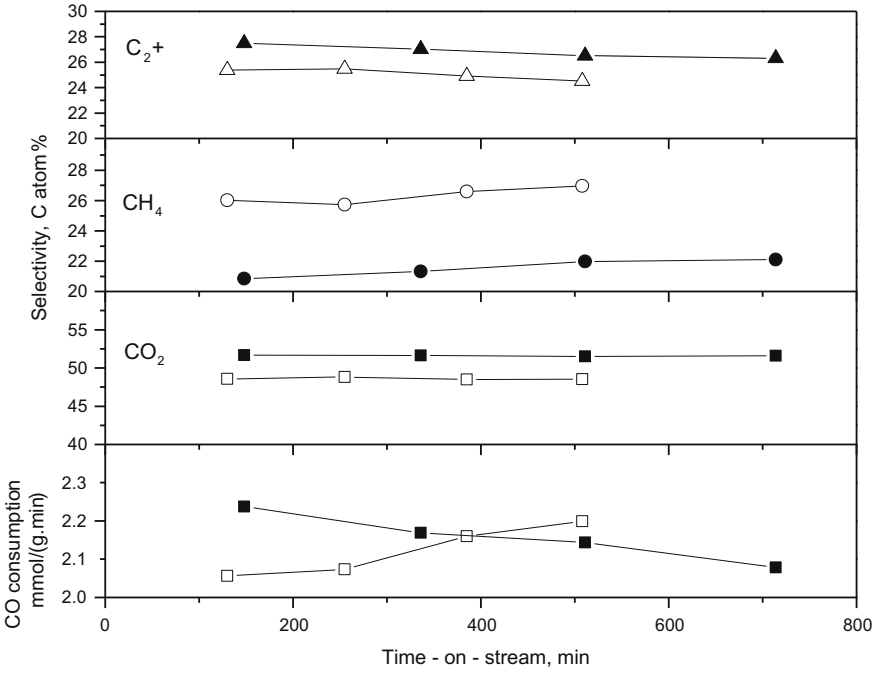


**Fig. 6.** CO consumption rate and product selectivities obtained over the un-treated $Mo_2C$ (open symbols) and the 2 h alkali-treated $Mo_2C$ (solid symbols) measured at 8.2 MPa, 573 K, $CO:H_2 = 1$ and GHSV = 3960 $h^{-1}$.

alkali metal to reduce selectivity to $CH_4$ so the high selectivity obtained in the present work was not unexpected. The alkali-treated catalysts had been thoroughly washed prior to use and EDX confirmed that the $Mo_2C$ was Na-free. The product distribution also showed enhanced water–gas-shift activity on the alkali-treated sample compared to the un-treated $Mo_2C$. Fig. 6 shows the change in CO consumption rate and the product selectivity obtained over a period of approximately 10 h. The product selectivities remained relatively constant during the experiments, whereas the alkali-treated catalyst showed some deactivation, possibly because of carbon deposition. A loss in activity in the first 2 h of reaction may also explain why the differences in the CO consumption rates between the un-treated and alkali-treated $Mo_2C$ were not as great as observed for the THCZ dehydrogenation reaction.

## 4. Conclusion

The surface area of an unsupported $Mo_2C$ catalyst was increased by a simple alkali-treatment of the $Mo_2C$ that had been prepared by temperature-programmed reaction of a $MoO_3$ precursor. The alkali-treatment increased the catalyst surface area by 50%, primarily through the creation of new pores of size <3 nm. The alkali-treatment did not change the $Mo_2C$ morphology nor the catalyst composition. The alkali-treated $Mo_2C$ showed enhanced activity for the dehydrogenation of THCZ and for CO hydrogenation, compared to the un-treated $Mo_2C$.

## Acknowledgement

Funding for the present study from Natural Sciences and Engineering Research Council of Canada is gratefully acknowledged. L.Z. thanks the Ministry of Education of China for scholarship support.

## References

[1] S.T. Oyama, Catal. Today 15 (2) (1992) 179–200.
[2] M. Espinnoza, J. Cruz-Reyes, M.D. Valle-Granados, E. Flores-Aquino, M. Avalos-Borja, S. Fuentes-moyado, Catal. Lett. 120 (1–2) (2008) 137–142.
[3] S.B. Derouane-Abd Hamid, J.R. Anderson, I. Schmidt, C. Bouchy, J.H. Jacobsen, E.G. Derouane, Catal. Today 63 (2–4) (2000) 461–469.
[4] C. Bouhy, S.B. Derouane-Abd Hamid, E.G. Derouane, Chem. Commun. 2 (2000) 125–126.
[5] S.Z. Li, J.S. Lee, T. Hyeon, K.S. Suslick, Appl. Catal. A 184 (1) (1999) 1–9.
[6] M. Nagai, T. Miyao, T. Tuboi, Catal. Lett. 18 (1993) 9–14.
[7] G. Djega-Mariadassou, M. Boudart, G. Bugli, C. Sayag, Catal. Lett. 31 (1995) 411–420.
[8] M. Xiang, D. Li, H. Qi, W. Li, B. Zhong, Y. Sun, Fuel 86 (9) (2007) 1128–1303.
[9] V. Keller, P. Weher, F. Garin, R. Ducros, G. Maire, J. Catal. 153 (1) (1995) 9–16.
[10] M. Nagai, A.M. Zahidul, K. Matsuda, Appl. Catal. A: General 313 (2) (2006) 137–145.
[11] A. Szechenyi, F. Solymosi, J. Phys. Chem. C 111 (26) (2007) 9509–9515.
[12] J.S. Lee, L. Volpe, F.H. Ribeiro, M. Boudart, J. Catal. 112 (1) (1988) 44–53.
[13] T.C. Xiao, A.P.E. York, V.C. Williams, H. Al-Megren, A. Hanif, Z.-Y. Zhou, M.L.H. Green, Chem. Mater. 12 (12) (2000) 3896–3905.
[14] X. Li, D. Ma, L. Chen, X. Bao, Catal. Lett. 116 (1–2) (2007) 63–69.
[15] J.M. Giraudon, L. Leclercq, G. Leclercq, A. Lofberg, A. Frennet, J. Mater. Sci. 28 (1993) 2449–2454.
[16] D. Zeng, M. Hampden-Smith, J. Chem. Mater. 5 (1993) 681–689.
[17] L.G. Rosa, J.C. Fernandes, P.M. Amaral, Int. J. Refract. Met. Hard Mater. 17 (1999) 351–356.
[18] P.M. Patterson, T.K. Das, B.H. Davis, Appl. Catal. A 251 (2003) 449–455.
[19] M.K. Neylon, S. Choi, H. Kwon, K.E. Curry, L.T. Thompson, Appl. Catal. A 183 (1999) 253–263.
[20] J.B. Claridge, A.P.E. York, A.J. Brungs, M.L.H. Green, Chem. Mater. 12 (2000) 132–142.
[21] M. Ogura, S. Shinomiya, J. Tateno, Y. Nara, M. Nomura, E. Kikuchi, M. Matsukata, Appl. Catal. A 219 (2001) 33–43.
[22] T. Suzuki, T. Okuhara, Microporous Mesoporous Mater. 43 (2001) 83–89.
[23] J.C. Groen, L.A.A. Peffer, J.A. Moulijn, J. Pérez-Ramírez, Colloids Surf. A: Physicochem. Eng. Aspects 241 (2004) 53–58.
[24] J.C. Groen, L.A.A. Peffer, J.A. Moulijn, J. Pérez-Ramírez, Microporous Mesoporous Mater. 69 (2004) 29–34.
[25] L.L. Su, L. Liu, J.Q. Zhuang, H.X. Wang, Y.G. Li, W.J. Shen, Y. Xu, X.H. Bao, Catal. Lett. 91 (3–4) (2003) 155–167.
[26] P. Crawford, R. Burch, C. Hardacre, K.T. Hindle, P. Hu, B. Kalirai, D.W. Rooney, Approach J. Phys. Chem. 111 (2007) 6434–6439.
[27] K.T. Hindle, R. Burch, P. Crawford, C. Hardacre, P. Hu, B. Kalirai, D.W. Rooney, J. Catal. 251 (2007) 338–344.
[28] F. Sotoodeh, L. Zhao, K.J. Smith, Appl. Catal. A 362 (2009) 155–162.
[29] M. Xiang, D. Li, W. Li, B. Zhong, Y. Sun, Catal. Commun. 8 (2007) 513–518.
[30] M. Xiang, D. Li, W. Li, B. Zhong, Y. Sun, Catal. Commun. 8 (2007) 503–507.
[31] M. Xiang, D. Li, H. Xiao, J. Zhang, W. Li, B. Zhong, Y. Sun, Catal. Today 131 (1–4) (2008) 489–495.
[32] F. Sotoodeh, K.J. Smith, Ind. Eng. Chem. Res., in press, doi:10.1021/ie9007002.